

*Full Length Research Paper*

# Planetary milling parameters optimization for the production of ZnO nanocrystalline

O. M. Lemine<sup>1,2\*</sup>, M. A. Louly<sup>3</sup> and A. M. Al-Ahmari<sup>3</sup>

<sup>1</sup>Physics Department, College of Sciences, Al-imam University, P. O. Box 90950, 11623 Riyadh, Kingdom of Saudi Arabia.

<sup>2</sup>School of Physics and Astronomy, University of Nottingham, Nottingham, NG7 2RD, United Kingdom.

<sup>3</sup>Princess Fatimah Alnijris's Research Chair for AMT, Industrial Engineering, Department, College of Engineering, King Saud University, Riyadh 11421, Saudi Arabia.

Accepted 1 December, 2010

**An artificial-neural-network (ANN) model is developed for the analysis and prediction of correlations between processing planetary milling parameters and the crystallite size of ZnO nanopowder by applying the back-propagation (BP) neural network technique. The input parameters of the BP network are rotation speed and ball-to-powder weight ratio. The nanopowder was synthesized by planetary mechanical milling and the required data for training were collected from the experimental results. The synthesized ZnO nanoparticles were characterized by X-ray diffraction (XRD) and Scanning Electron Microscopy (SEM). The crystallite size and internal strain were evaluated by XRD patterns using Williamson – Hall method. It was found that, artificial neural network was very effective providing a perfect agreement between the outcomes of ANN modeling and experimental results. An optimization model is then developed through the analysis on the evaluated network response surface and contour plots to find the best milling parameters (rotation speed and balls to powder ratio) producing the minimal average crystallite size.**

**Key words:** Milling, optimization, neural network, ZnO.

## INTRODUCTION

Various techniques have been used to synthesize ZnO nanoparticles and can be categorized into either chemical or physical methods (Klabunde, 2001). For example, hydrothermal (Ni et al., 2005), solvothermal (Wang et al., 2005), sol-gel (Ristic et al., 2005), direct chemical synthesis (Wu et al., 2006) and ball milling (Damonte et al., 2004), etc. Among these synthetic routes, Mechanical milling has proved to be an effective and simple technique, to produce nanocrystalline powders and the possibility of obtaining large quantities of materials. However, properties of nanopowders obtained by milling method are affected by various parameters such as milling time, ball to powder mass ratio, rotation speed, balls diameters, etc. Several groups were interested by

ball milling process modeling, mainly based on the mechanistic (Abdellaoui and Gaffet, 1995) and D'Incau et al. (2007), and thermodynamic (Badmos and Bhadeshia, 1997), Lu et al. (1997) and Suryanarayana (2001); approaches to achieve a general understanding at the atomic and phenomenological level.

Recently, Artificial Neural Network (ANN) becomes one of the most powerful modelling techniques, in conjunction with the statistical approach. It is suitable for simulations of the correlations which are hard to be described by physical models (Sha and Edwards, 2007). The advantages of ANN modeling are reduction of time and cost in all the required experimental activities. It can be used for the prediction of the mechanical milling outputs. However, there only limited work on the application of neural networks in the field of mechanical milling (Dashtbayazi et al., 2007) and Maa et al. (2009). The aim of this work is to develop a neural network model to the prediction and optimization of the planetary ball milling

\*Corresponding author. E-mail: [leminej@yahoo.com](mailto:leminej@yahoo.com), [mamamin@imamu.edu.sa](mailto:mamamin@imamu.edu.sa).

process for synthesizing ZnO nanocrystalline. The process parameters, including milling times, rotation speed and ball-to-powder mass ratio are applied to the neural network inputs, to provide information relating to crystallite size. The network is then trained to output the prediction on the powders particles size. An optimization model is then developed to find the best parameters producing the minimal average crystallite size.

## EXPERIMENTAL

### Samples preparation

Commercially, ZnO powders with average particle size of about 1  $\mu\text{m}$  and 99.9% of purity were introduced into a planetary milling – “PULVERISSETTE 7 premium line”. The bowls and balls made of Zirconia to avoid contamination were used. The powder was ground in vial with 2 g of ZnO and mixture of Zirconia balls (10 and 15 mm in diameter). The rotation speed and balls to powders mass ratio were varied in the range of 300 to 400 rpm and 10 to 20 respectively.

### Structural characterization

X-ray powder diffraction (XRD) measurements were performed using Shimadzu diffractometer ( $\theta$ - $2\theta$ ) equipped with Cu-K $\alpha$  radiation ( $\lambda=1.5418$  Å). It is known that X-ray diffraction line broadening is influenced by the particles size and the internal strains. In order to obtain these parameters, Williamson – Hall was used and the analysis includes two steps:

First step: The width ( $\beta_{\text{exp}}$ ) of every peak was measured as the integral breadth. The instrumental broadening ( $\beta_{\text{inst}}$ ) was determined from polycrystalline silicon standard. The peak breadth due to sample (strain + size), B was calculated according to Gaussian profile:

$$B^2 = \beta_{\text{exp}}^2 - \beta_{\text{inst}}^2 \quad (1)$$

Second step: The crystalline size and internal strain were obtained by fitting the Williamson – Hall equation:

$$B \cos \theta = \frac{K\lambda}{D} + 2\varepsilon \sin \theta \quad (2)$$

Where D is the coherent scattering length (crystalline size);  $\lambda$  is the wave length used,  $\theta$  the bragg reflection peak, K is a constant whose value is approximately 0.9; B the integral width of the sample (in rad) calculated in the first step and  $\varepsilon$  the inhomogeneous internal strain (in %). Particles morphology was investigated using Nova 200 NanoLab field emission scanning electron microscope (FE-SEM).

### Neural networks modeling procedure

Artificial neural networks provide a mapping of inputs to outputs and consist of computer programs based on the structure of brain. As such, they can be trained to recognize patterns within data. In the human brain, a neuron is a nerve cell which processes incoming information and outputs a signal to the relevant part of the body accordingly. Some inputs are stronger than the others, that is, they are 'weighted'. The total effect of the inputs is the sum of the

weighted signals, and, if this exceeds the neuron threshold, a response is produced. By comparison, in an artificial neural network, a number of inputs are applied simultaneously, via weighted links, and the node calculates a combined total input. The relation between the input and output is specified by a transfer or activation function, which describes the threshold for deciding on the state of the output of that particular node. A number of nodes may be combined to form a layer, and layers may be interconnected to form a complete network. The procedure of designing the neural network architecture is described in detail as follows.

## RESULTS AND DISCUSSION

### Characterization of ZnO nanopowder

Figure 1 represents the evolution of XRD patterns of ZnO powder for the samples prepared under different milling condition such as balls to powder ratio, time milling and rotation speed. It can be shown that, all Bragg peaks of the XRD patterns showed only the ZnO reflections, indicating that, there is no phase transformation during the milling have occurred. With increasing balls to powder ratio and rotation speed, the diffraction peaks became broader and their relative intensity decreases. This effect is typical behavior of materials after milling and attributed usually to the presence of particles with small size and internal strain induced by mechanical deformation. It is well known that the peak broadening can be caused by both a reduction in crystallite size and an increase in lattice strain. For a quantitative comparison, the physical broadenings for the sample with balls to powder mass ratio of 10:1 are presented in Figure 2. It can be observed that, broadenings of breadth peaks increase with rotation speed. The variation of the integral breadth vs. diffraction angle shown in Figure 2 can be related to the Bragg's angle effect.

The crystallite size and internal strain were estimated from the Williamson-Hall method. The five most intensive reflection peaks of the samples were used in the line broadening analysis. Figure 3 shows Williamson-Hall plot for sample with balls to powder ratio (10:1) and rotation speed of 300 rpm. From this curves we can estimate the crystalline size (intercept at  $\sin\theta = 0$ , from the Equation 2), and internal strain (slop). The results are summarized in Table 1. Figure 4 shows the evolution of crystallite size with rotation speed for different balls to powder mass ratio. For increasing rotation speed and for different ball to powder ratio, the crystallite size decreases, while the internal strain increases (Figure 5). This behaviour is explained by the formation of defects during the milling process. The evolution of crystallite size with rotation speed can be divided in three stages:

1. For rotation speed of 300 rpm, the crystallite size decrease with increasing balls to powders ratio.
2. For rotation speed of 350 rpm, the crystallite size obtained for balls to powder ratio of 10 is lower than that

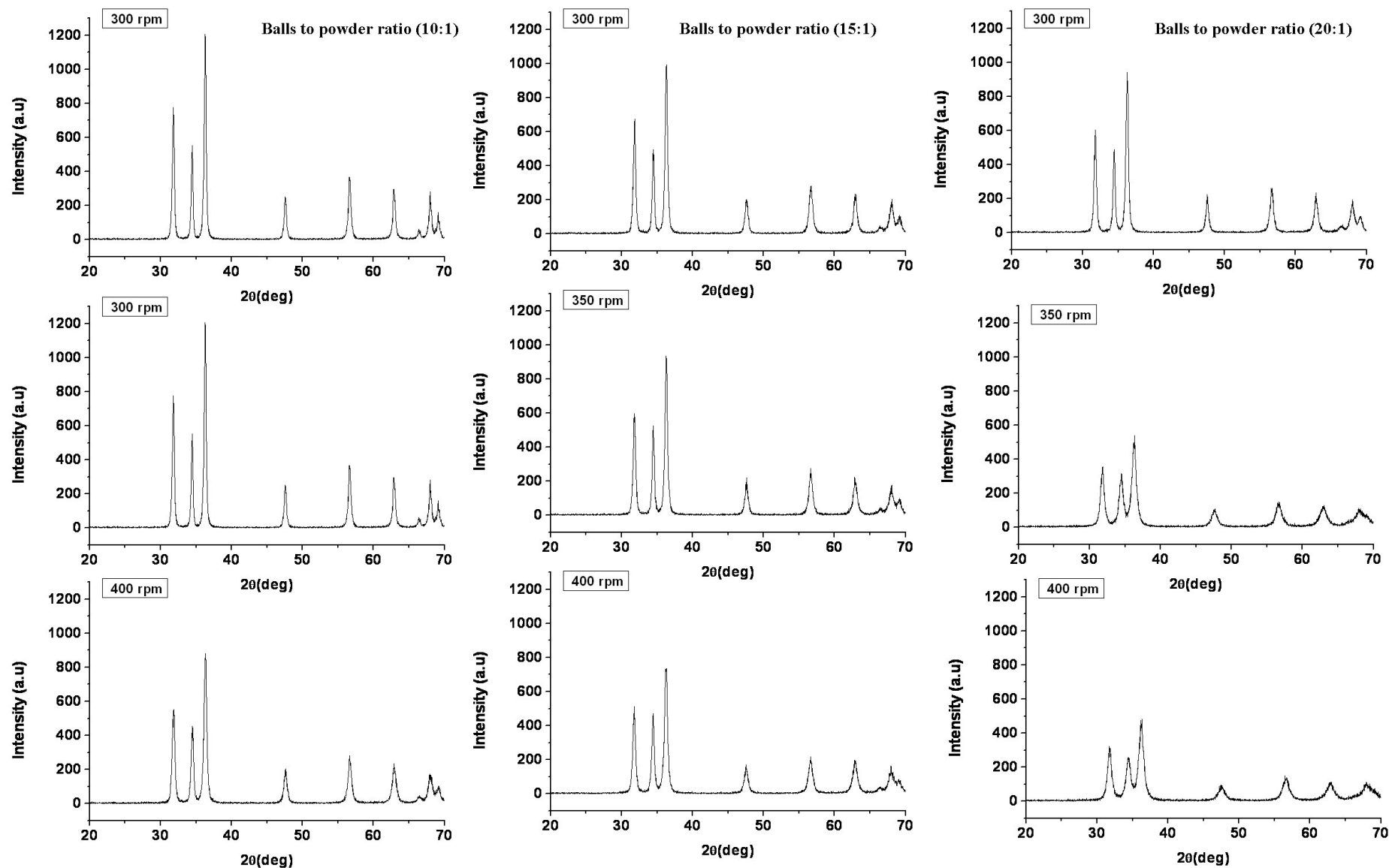
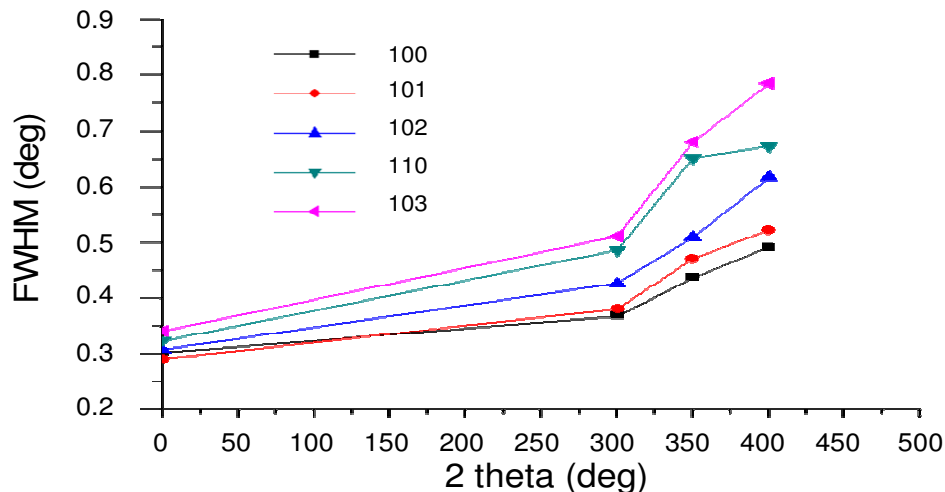
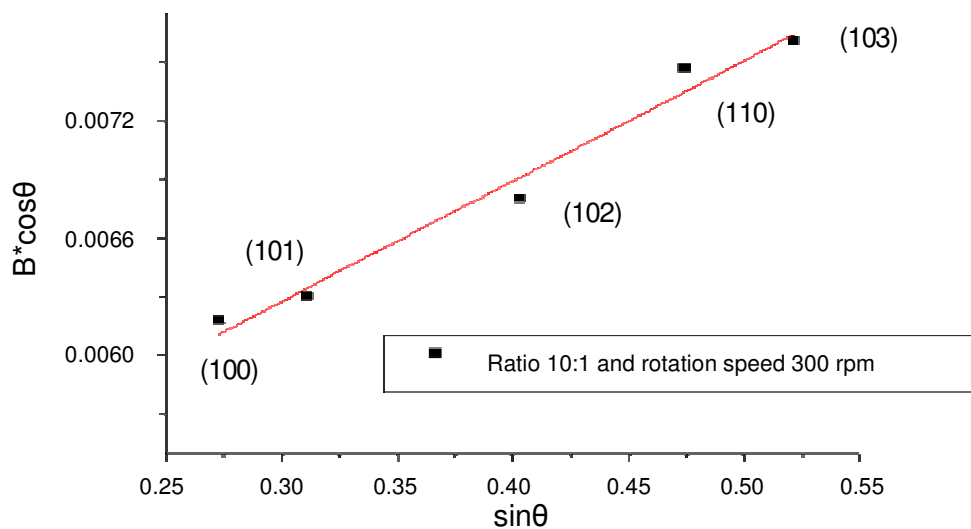


Figure 1. X-ray diffraction patterns for ZnO powders milled for 5 h and for different balls to powder ratio.



**Figure 2.** Change in the integral breadth of the samples milled at different rotation speed.



**Figure 3.** An example of Williamson –Hall plot showing X-ray peak broadening (B) as function of Bragg angle ( $\theta$ ) for the sample: balls to powder ratio (10:1) and rotation speed of 300 rpm.

**Table 1.** Crystallite size and internal strain values.

Balls to powder mass ratio (R = balls weight/powder weight)	Rotation speed	Crystallite size (nm)	Internal strain (%)	Times milling (h) TM
10	300	25.5	0.003	
10	350	19.6	0.005	
10	400	17.6	0.006	
15	300	20.18	0.006	
15	350	20.5	0.009	5 h
15	400	16	0.01	
20	300	20	0.007	
20	350	12	0.018	
20	400	10	0.003	

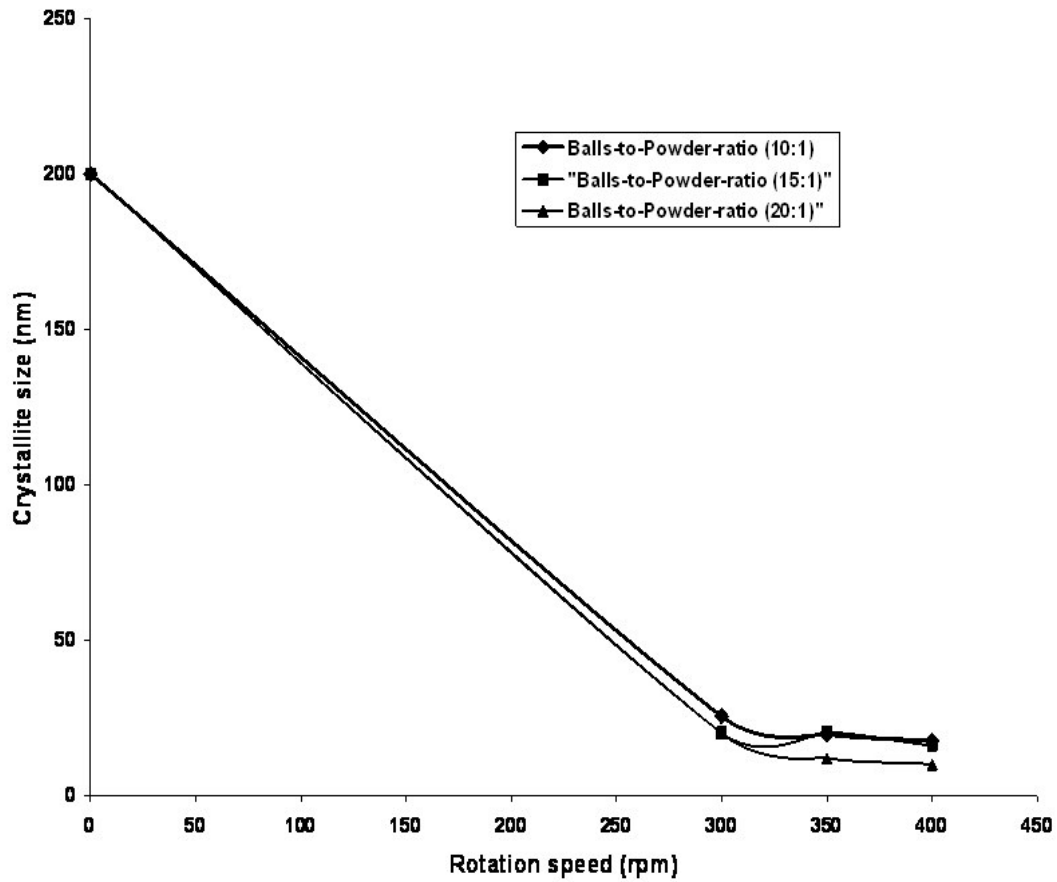


Figure 4. Evolution of crystalline size as function of rotation speed and balls to powder ratio.

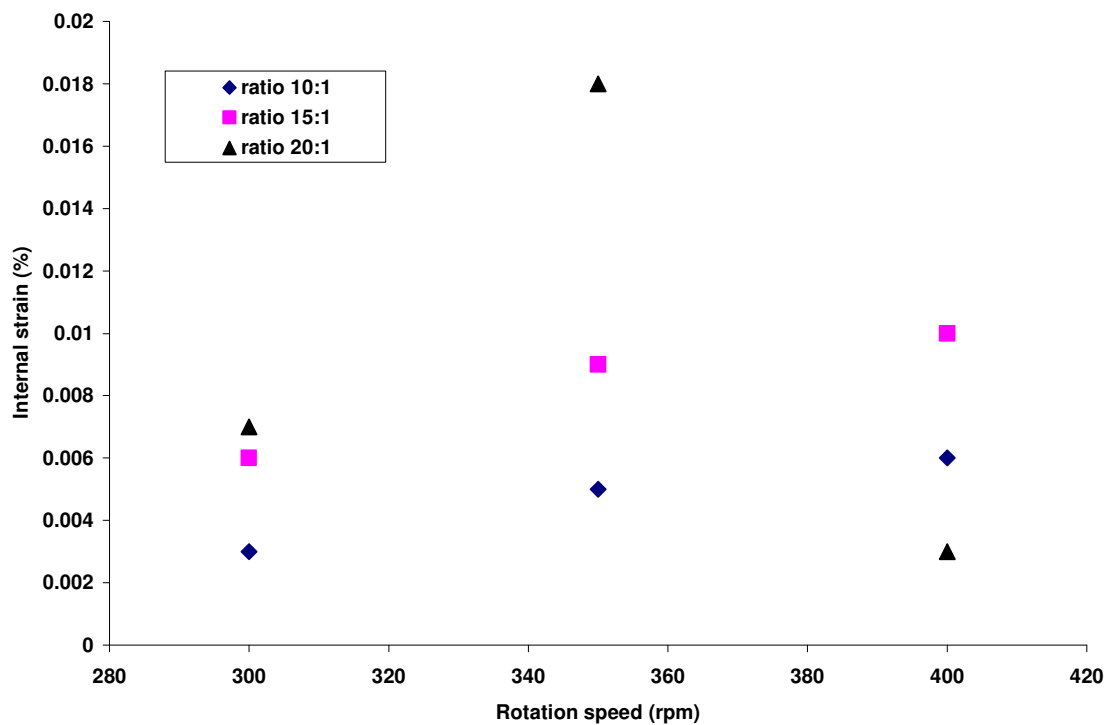


Figure 5. The variation of internal strain with the ratio speed and balls to powder mass ratio.

obtained for balls to powder ratio of 15.

3. For rotation speed of 400, again the crystallite size decrease with increasing balls to powders ratio.

Similar behavior has been reported in previous work (Lemine et al., 2009; Damonte et al., 2004). In their studies, a clear reduction of grain size and increase of the internal strain for longer milling times of ZnO powder were observed. However, only in this current work the internal strain decreases at 400 rpm for ratio of 20:1. This phenomenon can be explained by annealing effect during milling. If the grain size reached its saturation value, the impact of milling is to anneal the highly stressed particles (Bégin-Colin et al., 2000). As a result, the lattice strain decreases or remains constant. A same phenomenon was observed in the milling of hematite nanocrystalline (Lemine, 2009). Another difference with previous work is that, the time milling was fixed and others milling parameters (balls to powders ratio and rotation speed) were modified but the same effects are produced.

SEM micrographs of the samples rotation speed of 400 rpm and for different balls to powder mass ratio are shown in Figure 6. It is clear that after milling, a reduction of the crystalline size can be observed with relatively better homogeneity. High magnification images (right) reveal clearly that, large particles are in fact agglomerates of much smaller particles.

### Artificial neural networks simulator

An artificial neural network simulator has been developed, to find out the relationship between the experience's inputs (the mass ratio of ball to powder and the rotation speed) and the experience's output (the average particles size). A multi-layer perceptron with back propagation training has been implemented on MATLAB. The network is composed of 3 layers. There are 6 nodes in the input layer corresponding respectively to Ratio (R), Speed (S), R\*R, S\*S, R\*S, and the constant coefficient, which is set equals to one. There is only one node in the output layer corresponding to the particles size (PS). There is one hidden layer composed of 6 nodes. The tanh is used as activation function for the hidden layer. Figure 7 illustrates this network's architecture.

This artificial neural network was trained using the retropropagation algorithm that minimizes the mean squared error over a training set of 8 experiences as given in Table 2. This training algorithm was efficient. In few seconds, the mean squared error has reached almost zero. The steady state is given by two matrixes. The first 2-dimension matrix, representing the input weights that connect the input layer to the hidden layer, is as follows:

1.7354 -0.1161 1.2265 -0.4221 -1.4681 -1.9683

-0.0645 -1.9287 1.0436 1.8058 -0.6235 1.0526  
0.3221 1.4076 -1.8150 -1.9193 -1.3368 -0.0809  
0.9154 -0.2033 -0.3074 -0.3687 0.8175 1.8338  
1.8942 0.5128 1.6107 1.2831 -0.7151 -0.1424  
1.4629 0.7562 0.2426 -1.3742 -0.3230 -1.1312

The second 1-dimension matrix, representing the hidden weights that connect the hidden layer to the output node, is as follows:

1.3477 -0.5214 -1.2066 0.7726 1.6688 -1.3457

The particle size is then given by the following formula:

$$PS_{net} = \sum_{j=1}^6 w_j \tan\left(w_j R + w_j S + w_j R^2 + w_j S^2 + w_j R S + w_j\right)$$

Where  $w_i$  and  $w_h$  are respectively the input and hidden weights. The inputs  $x_i$  are R, S, R\*R, S\*S, R\*S, and 1. The obtained value is multiplied by the standard deviation and added to the mean, as input data were normalized in order to speed up the training algorithm.

In order to assess the validity of the networks and their accuracy, it is often useful to perform regression analysis between the network response and the corresponding target. This artificial neural network was very effective providing a perfect link between the inputs and the outputs. In fact, using MINITAB software, we find the following multiple regression coefficients:

$$PS_{reg} = 54 - 0.69Ratio - 0.0736Spec$$

The mean absolute deviation obtained with this regression is 1.46.

The results of the regression are shown in Table 2. It's is clear from that there is a consistence agreement between the outcomes of ANN modeling and experimental results as well as the current knowledge of mechanical milling process exists. It is noted also that, the error obtained by ANN model is by far better than multiple linear regressions.

This agreement between the outcomes of ANN and experiments was obtained by (Dashtbayazi et al., 2007) and Maa et al. (2009) but in our model the relative errors was better. The difference in the errors between ours models can be explained by the numbers of output parameters. In our model we were only interested by the crystallite size parameters. For their models the output was strain and crystallite size. It is interesting also to note that in our work planetary milling machine was used (they used vibrant milling). After constructing the ANN model and evaluating its accuracy and modeling error by regression analysis and total error estimation of the ANN network, one can use this network for prediction and optimization of the planetary mechanical milling process

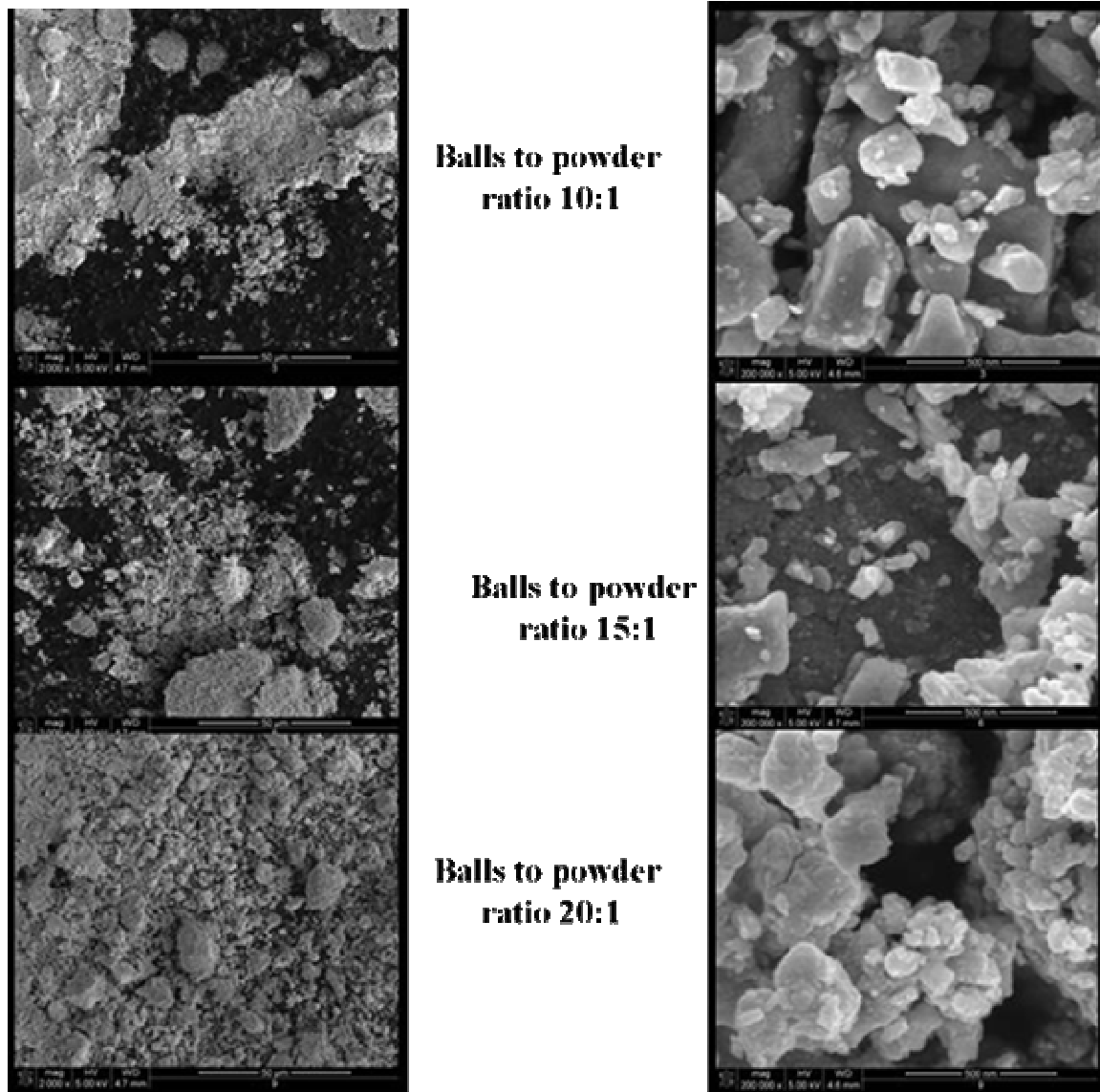


Figure 6. SEM of milled ZnO powder for rotation speed of 400 rpm: Low magnification (left) and high. magnification (right).

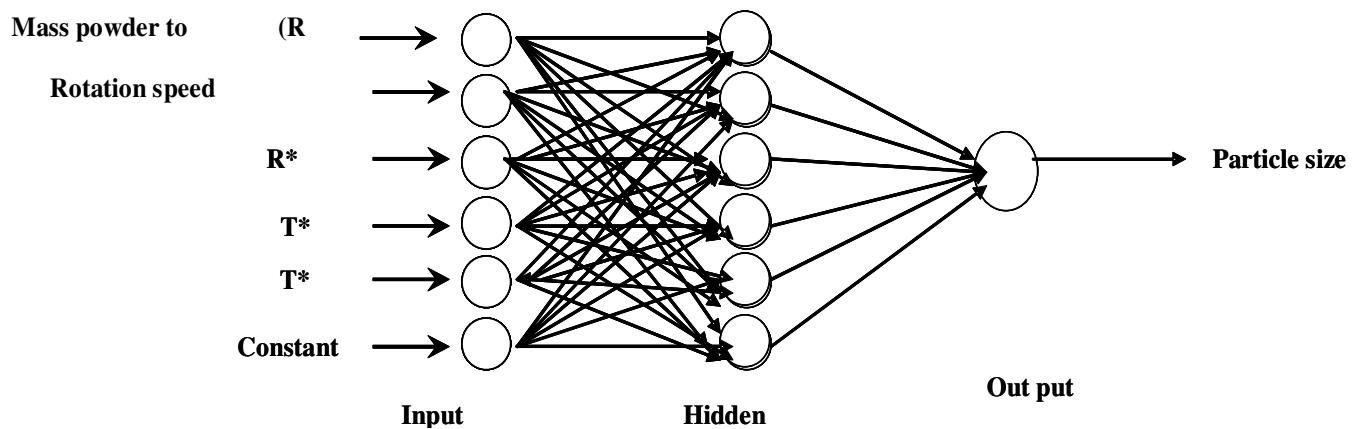
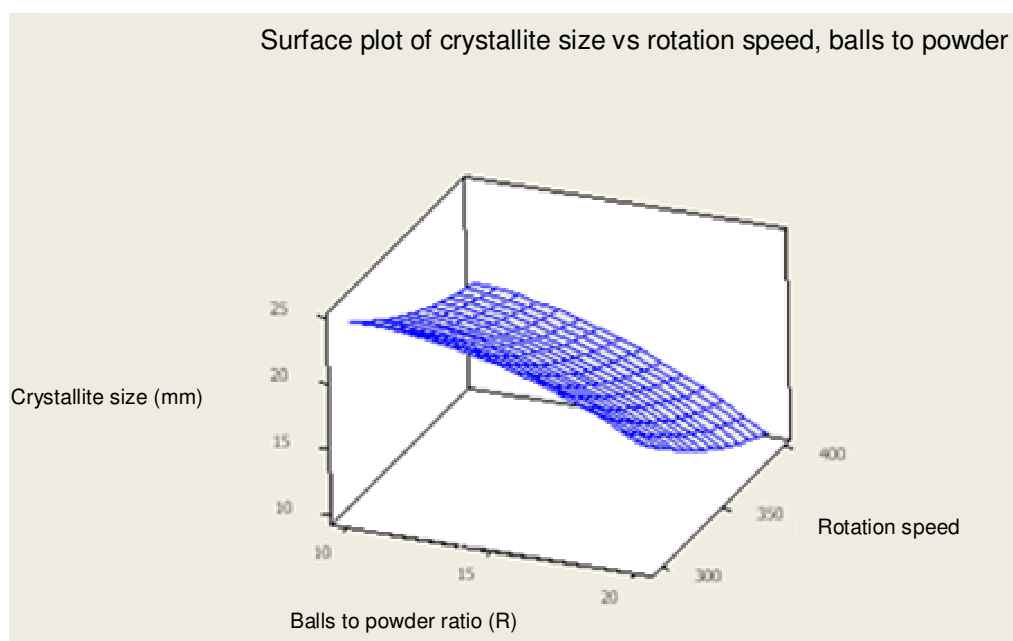


Figure 7. The artificial neural network.

**Table 2.** Comparison between the network and regression estimations.

Experimental particles size (nm)	Network estimations	Regression estimation
25.5	25.5	25.02
19.6	19.6	21.34
17.6	17.6	17.66
20.18	20.18	21.57
20.5	20.5	17.89
16	16	14.21
20	20	18.12
12	12	14.44
10	10	10.76

**Figure 8.** Surface responses of particle size.

for synthesizing of ZnO nanopowders.

Figure 8 shows the response surfaces of powder properties with the milling parameters. In order to clarify the response surfaces, contour plots for the crystallite size of the ZnO nanopowders in terms of the milling parameters (balls to powder ratio and rotation speed) is demonstrated in Figure. 9. There is only one region where the crystallite size is in the minimum level (about 12 to 16 nm) with the high rotation speed ( $v \geq 360$  rpm) and large balls to powder ratio (20:1). A similar result was found by Maa et al. (2009) for the mechanically alloyed WC–18 at %MgO nanocomposite powders. They obtained a small crystallite size for higher rotation ( $v \geq 300$  rpm) speed and for balls diameter ( $d \geq 8$ mm). Some experiments will be conducted in the future in order to validate the above parameters obtained from the optimization.

## Conclusions

An artificial-neural-network (ANN) model was developed to estimate the crystallite size of ZnO nanopowders, as a function of the planetary milling parameters (rotation speed and balls to powder ratio). It was found that artificial neural network model was very effective, providing a perfect agreement between the outcomes of ANN modeling and experimental results.

Furthermore, the optimization of the planetary milling process for fabricating the nanocrystalline ZnO powder, is carried out through the analysis on the evaluated network response surface and contour plots. The optimized milling parameters were rotation speed ( $350 \text{ rpm} < v \leq 400 \text{ rpm}$ ) and balls to powder ratio (20:1). In addition, the neural network model developed can be used for the prediction of other parameters such as strain, lattices

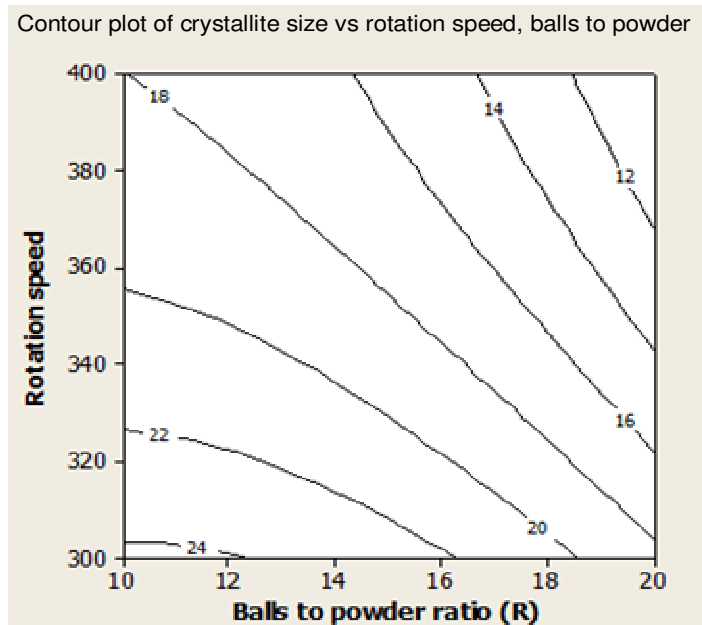


Figure 9. The contour plot of crystallite size.

parameters.

## ACKNOWLEDGEMENTS

This work was supported by the Center of Excellence for Research in Engineering Materials (CEREM), King Saud University.

## REFERENCES

- Abdellaoui M, Gaffet E (1995). The Physics of Mechanical Alloying in a Planetary. Ball Milling: Mechanical Treatment. *Acta. Metal Mater.*, 43: 1087–1098.
- Badmos AY, Bhadeshia HKDH (1997). The evolution of solutions: A thermodynamic analysis of mechanical alloying. *Metal Mater. Trans.*, 28A: 2189–2194.
- Bégin-Colin S, Girot T, Le Caer G, Mocellin A (2000). Kinetics and Mechanisms of Phase Transformations Induced by Ball-Milling in Anatase TiO<sub>2</sub>. *J. Solid State Chem.*, 149(1): 41–48.
- D'Incau M, Leoni M, Scardi P (2007). High-energy grinding of FeMo powders. *J. Mater. Res.*, 22: 1744–1753.
- Damonte LC, Mendoza Zelis LA, MariSoucase B, Hernandez Fenollos MA (2004). Nanoparticles of ZnO obtained by mechanical milling. *Powder Technol.*, 148: 15–19.
- Dashtbayazi MR, Shokuhfar A, Simchi A (2007). Artificial neural network modeling of mechanical alloying process for synthesizing of metal matrix nanocomposite powders. *Mater. Sci. Eng. A*, 466: 274–283.
- Klabunde KJ (2001). *Nanoscale Materials in Chemistry*, p.88, John Wiley and Sons, New York, 88: 3535–3537.
- Lemine OM (2009). Microstructural characterisation of  $\gamma$ -Fe<sub>2</sub>O<sub>3</sub> nanoparticles using, XRD line profiles analysis, FE-SEM and FT-IR, *Superlattices and Microstructures*, 45: 576–582.
- Lemine OM (2009). Effects of milling time on the formation of nanocrystalline ZnO. *Int. J. Nanoparticles*, 2: 1/2/3/4/5/6.
- Lu L, Lai MO, Zhang S (1997). Diffusion in mechanical alloying. *J. Mater. Proc. Technol.*, 67: 100–104.
- Maa J, Zhu SG, Wu CX, Zhang ML (2009). Application of back-propagation neural network technique to high-energy planetary ball milling process for synthesizing nanocomposite WC–MgO powders. *Mater. Design*, 30: 2867–2874.
- Ni YH, Wei XW, Hong JM, Ye Y (2005). Hydrothermal and optical properties of ZnO nanorods. *Mater. Sci. Eng. B*, 121: 42–47.
- Ristic M, Music S, Ivanda M, Popovic S (2005). Mismatch strain induced formation of ZnO/ZnS heterostructured rings. *J. Alloy Compd.*, 397: L1–L4.
- Sha W, Edwards KL (2007). The use of artificial neural networks in materials science based research. *Mater Design*, 28: 1747–1752.
- Suryanarayana S (2001). Mechanical alloying and milling. *Prog. Mater. Sci.*, 46: 1–184.
- Wang C, Shen E, Wang E, Gao L, Kang Z, Tian C, Lan Y, Zhang C (2005). Controllable synthesis of ZnO nanocrystals via a surfactant-assisted alcohol thermal process at a low temperature. *Mater. Lett.*, 59: 2867–2871.
- Wu C, Qiao X, Chen J, Wang H, Tan F, Li S (2006). A novel chemical route to prepare ZnO nanoparticles. *Mater. Lett.*, 6: 1828–1832.